Journal of Applied Phycology
https://doi.org/10.1007/s10811-024-03291-1

RESEARCH

Modeling the growth of the cultivated seaweed *Undaria pinnatifida* under climate change scenarios in the Seto Inland Sea, Japan

Goh Onitsuka[1] · Goro Yoshida[2] · Hiromori Shimabukuro[1] · Shoichi Takenaka[3,8] · Toshiharu Tamura[3,9] · Shigeho Kakehi[4] · Takashi Setou[5] · Xinyu Guo[6] · Hironori Higashi[7]

Received: 13 March 2024 / Revised: 14 May 2024 / Accepted: 30 May 2024

Abstract

To assess the potential effects of future climate change on *Undaria pinnatifida* cultivation in the Seto Inland Sea, Japan, we developed an individual-based growth model for the *U. pinnatifida* sporophyte. Initially, we validated the model's performance using field observation data. The simulation results replicated temporal variations in the total lengths of sporophytes at two stations with differing oceanographic conditions. Subsequently, we conducted numerical simulations of sporophyte growth in the Seto Inland Sea during the 1990s and projected outcomes for the 2090s under four emission scenarios of the Representative Concentration Pathway (RCP 2.6, 4.5, 6.0, and 8.5). The majority of areas exhibited decreased sporophyte growth in the 2090s compared to the 1990s, except for the eastern area under the RCP 2.6 scenario. This decline was attributed to delayed cultivation start times associated with ocean warming and reduced dissolved inorganic nitrogen concentrations. Interestingly, the impacts of ocean warming on *U. pinnatifida* cultivation were not uniformly negative. In addition to adverse effects, there were positive effects that accelerated growth rates in low-temperature winter areas. Sensitivity analyses revealed that the balance between positive and negative impacts varied geographically; moreover, the contrasts were enhanced with higher RCP scenarios. Simulations for climate change adaptation using a high-temperature tolerant cultivar indicated that yield losses could be mitigated, even under the RCP 8.5 scenario. Despite uncertainties in the simulation results, such as future management of nutrient loads and herbivore feeding damages, our projections underscore the potential sustainability and future viability of *U. pinnatifida* aquaculture in the Seto Inland Sea.

Keywords Aquaculture · Phaeophyceae · Kelp · Sporophyte · Growth model · RCP scenarios · Adaptation

✉ Goh Onitsuka
onitsuka_go81@fra.go.jp

[1] Hatsukaichi Field Station, Fisheries Technology Institute, Japan Fisheries Research and Education Agency, Hatsukaichi, Hiroshima 739-0452, Japan

[2] Nagasaki Field Station, Fisheries Technology Institute, Japan Fisheries Research and Education Agency Nagasaki, Nagasaki 851-2213, Japan

[3] Ehime Research Institute of Agriculture, Forestry and Fisheries, Fisheries Research Center, Uwajima, Ehime 798-0104, Japan

[4] Shiogama Field Station, Fisheries Stock Assessment Center, Fisheries Resources Institute, Japan Fisheries Research and Education Agency, Shiogama, Miyagi 985-0001, Japan

[5] Yokohama Field Station, Fisheries Resources Institute, Japan Fisheries Research and Education Agency, Yokohama, Kanagawa 236-8648, Japan

[6] Center for Marine Environmental Study, Ehime University, Matsuyama, Ehime 790-8577, Japan

[7] Regional Environment Conservation Division, National Institute for Environmental Studies, Tsukuba, Ibaraki 305-8506, Japan

[8] Present Address: Biodiversity Center, Ehime Prefectural Institute of Public Health and Environmental Science, Toon, Ehime 791-0211, Japan

[9] Present Address: Fisheries Department, Chuyo Regional Office Ehime Prefecture, Matsuyama, Ehime 790-8502, Japan

Published online: 21 June 2024

Introduction

The annual production of seaweed has seen a rapid increase worldwide, largely due to the expansion of aquaculture. In 2020 it reached approximately 35 million tonnes, constituting 29% of total aquaculture production (FAO 2022). Seaweed farming is anticipated to serve multiple purposes, including food production, the extraction of nutritional compounds, and climate change mitigation (e.g.,Duarte et al. 2017; Wang et al. 2018; Froehlich et al. 2019; Ross et al. 2023; Sultana et al. 2023; Troell et al. 2023).

Among the various seaweed species, the large brown macroalga *Undaria pinnatifida* (Harvey) Suringar (Laminariales; Phaeophyceae) stands out as a major commercial seaweed native to the northwest Pacific. *U. pinnatifida* is rich in carbohydrates, proteins, microelements, and various secondary metabolites, with strong bioactivities (Wang et al. 2018). It is extensively cultivated as a seafood in East Asian countries such as Japan, Korea, and China (Yamanaka and Akiyama 1993). Since the 1970s, *U. pinnatifida* has invaded coastal regions worldwide, including Europe, North and South America, and Oceania (James et al. 2015; Epstein and Smale 2017). Recent report indicates cultivation in countries like France, Spain, Australia, and New Zealand (FAO and WHO 2022). The global annual production of *U. pinnatifida* reached approximately 2.8 million tonnes in 2020, accounting for 8% of total algal production (FAO 2022).

In Japan, large-scale cultivation of *U. pinnatifida* has been ongoing since the 1950s (Yamanaka and Akiyama 1993). One of the primary cultivation regions is the area surrounding the Naruto Strait, referred to as the Naruto area, situated in the eastern Seto Inland Sea (Fig. 1). In this area, the cultivation season for *U. pinnatifida* sporophytes extends from autumn to spring, primarily during the winter. Maintaining sufficient yields in the non-feeding aquaculture of *U. pinnatifida* relies heavily on oceanographic conditions, with water temperature being a critical factor. Juvenile sporophytes attached to seed ropes are transferred to the ambient sea area for nursery cultivation once the water temperature sufficiently decreases, as they are susceptible to high temperatures. It is recommended to start the culture at an ambient water temperature of 23°C to avoid physiological damage (Dan et al. 2015). An increase in water temperature may lead to a shortened culture period due to delays in aquaculture initiation, resulting in decreased yields (Tanada 2016; Yoshida et al. 2019). Additionally, nutrient deficiency in seawater can lead to withering and discoloration of *U. pinnatifida* sporophytes (Yoshikawa et al. 2001; Gao et al. 2013; Makino et al. 2015; Endo et al. 2017; Kakehi et al. 2018; Kaga et al. 2022), making nutrient concentration another crucial factor for sustainable cultivation of *U. pinnatifida*.

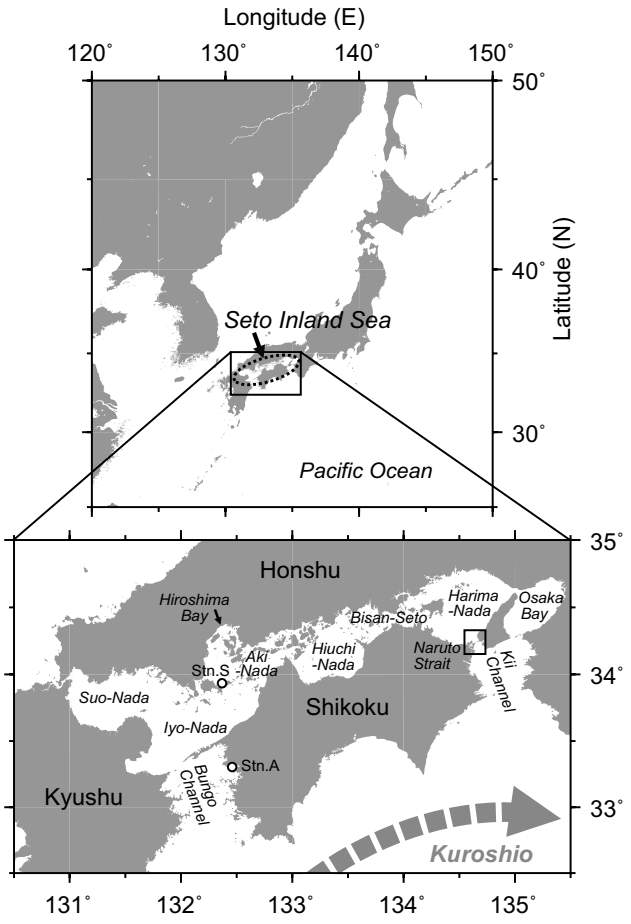

Fig. 1 Map of the study area in the Seto Inland Sea, Japan, depicting observation stations (Stns. A and S) with open circles

The Sixth Assessment Report (AR6) of the intergovernmental panel on climate change (IPCC) projects significant climate change impacts and various risks for coastal ecosystems by the end of the 21st century (IPCC 2022). In the Seto Inland Sea, a coupled hydrodynamic-biogeochemical model was used to predict oceanographic conditions in the 2090s under the Representative Concentration Pathway 8.5 (RCP8.5) scenario (Higashi et al. 2020). The study by Higashi et al. (2020) indicates that the winter water temperature in the 2090s in Harima-Nada, an area in the eastern Seto Inland Sea adjacent to the Naruto area, will rise by approximately 3°C compared to the 1990s. Additionally, the winter nutrient concentration is expected to be lower than that in the 1990s. From a long-term management perspective, predicting the impacts of these future oceanographic conditions on the cultivation of *U. pinnatifida* is a crucial step. This prediction will aid in devising appropriate countermeasures to ensure the sustainability of the aquaculture industry in the Seto Inland Sea.

Herein, we developed an individual-based growth model for the sporophyte of *U. pinnatifida* and applied it to the

Seto Inland Sea. Next, we simulated the seasonal growth of *U. pinnatifida* in the 1990s and 2090s under the present and future climate scenarios, respectively. Differences in growth dynamics among the areas were identified and sensitivities of environmental factors were evaluated using the growth model. In recent years, there have been several attempts to develop high-temperature tolerant cultivars as countermeasures for ocean warming (Tanada 2016; Niwa and Kobiyama 2019; Murase et al. 2021). Assuming that cultivations of high-temperature tolerant cultivars could be initiated earlier in the future climate conditions, compensating for the yield loss will be possible. Therefore, we conducted another simulation to evaluate the effect of countermeasure with a high-temperature tolerant cultivar as a tool for climate change adaptation.

Materials and methods

Study area

The Seto Inland Sea (SIS), Japan's largest semi-enclosed coastal sea, has an average depth of 38 m and encompasses over 700 small islands (Fig. 1). It is flanked by three large islands: Honshu, Kyushu, and Shikoku, and connects to the Pacific Ocean via the Bungo and Kii Channels. The sea features several basins, known as "Nada" in Japanese, which are linked by narrow channels called "Seto". The oceanographic conditions in the SIS exhibit significant horizontal contrasts, influenced by surface heat fluxes, freshwater inputs from rivers, and tidal currents that prevail around the narrow channels (Chang et al. 2009). The water quality in the area is affected by intrusions of offshore waters originating from the Kuroshio and the continental shelf through the Bungo and Kii Channels (Takeoka 2002; Yanagi and Ishii 2004; Kobayashi and Fujiwara 2009; Leng et al. 2023). Geographically enclosed sub-basins adjacent to densely populated watersheds, such as the inner part of Osaka Bay, exhibit relatively high concentrations of nutrients and chlorophyll *a* due to anthropogenic loads (Abo et al. 2018; Nishijima 2018; Higashi et al. 2020). The eastern SIS is the primary region for the cultivation of *U. pinnatifida*.

Growth model for sporophyte of *U. pinnatifida*

We developed an individual-based growth model for the sporophyte of *U. pinnatifida* to simulate seasonal growth influenced by environmental factors. While most laboratory experiments on *U. pinnatifida* growth have focused on changes in blade areas of young sporophytes to estimate relative growth rates (Morita et al. 2003; Baba et al. 2006; Baba 2008; Murase et al. 2021), our study utilized total length (TL) data from field observations conducted by Takenaka et al. (2021) to validate the model's performance. Due to the absence of blade area measurements in this dataset, we used the square of TL as a dependent variable. When TL and the width of the sporophyte have a linear relationship, the relative growth rate of the square of TL roughly corresponds to that of the blade area. The model incorporates environmental variables affecting sporophyte growth, including water temperature, nutrient concentration (specifically dissolved inorganic nitrogen: DIN), water motion (i.e., current speed), and cultivation density (i.e., insertion interval of seed rope to cultivation rope). Additionally, erosion at the blade tip was considered based on previous studies simulating brown macroalgae (Broch and Slagstad 2012; Zhang et al. 2016). The governing equations are as follows:

$$\frac{dL^2}{dt} = (\mu - \gamma)L^2 \tag{1}$$

$$\mu = f(T)f(N)f(U)f(D) \tag{2}$$

$$\gamma = f\left(L^2\right) \tag{3}$$

where L denotes the TL of the *U. pinnatifida* sporophyte in meters. The symbols μ and γ denote the rates of growth and erosion, respectively, per day. These rates are determined by several factors: water temperature (T: ℃), DIN concentration (N: μM), current speed (U: m s^{-1}), the insertion interval of the seed rope to the cultivation rope (D: m), and the square of TL (L^2: m^2).

The growth of the *U. pinnatifida* sporophyte is influenced by temperature, with an optimal range of 0℃–27℃. However, the optimum growth rate is site-specific, typically falling within 5℃–20℃ (Epstein and Smale 2017). Laboratory culture experiments have found that the optimum temperature for the growth of young sporophytes is approximately 15℃–20℃ (Morita et al. 2003; Baba 2008; Gao et al. 2013; Murase et al. 2021). Based on laboratory experiments with three strains from the east coast of Shikoku, including the Naruto cultivar (Murase et al. 2021), we set the function of water temperature as follows:

$$f(T) = \left(\frac{T}{T_{opt}}\right)^{\alpha T+\beta} \exp\left\{1 - \left(\frac{T}{T_{opt}}\right)^{\alpha T+\beta}\right\} \tag{4}$$

where T_{opt} represents the optimum temperature for growth, while α and β are constant values. The parameters of T_{opt} (17.37℃), α (0.078), and β (1.05) were derived using the least squares method with the *nls* function in R 4.0.4 (R Core Team 2021). The growth function indicates that maximum growth occurs at T_{opt}, and the growth rate decreases rapidly when the temperature exceeds 20℃ (Fig. 2). We assumed that the growth function depicted in Fig. 2 remained consistent throughout the sporophyte growth period.

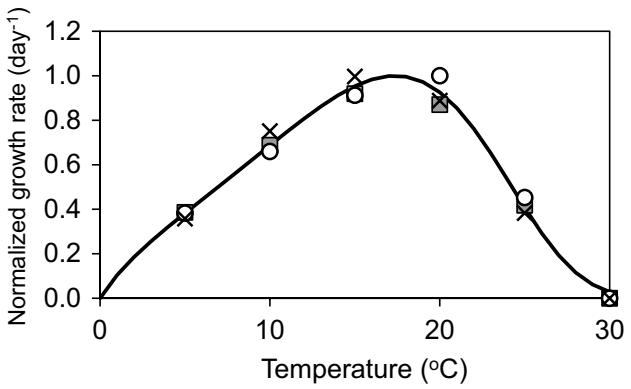

Fig. 2 Relationship between water temperature and the normalized growth rate of *Undaria pinnatifida* sporophyte derived from laboratory experiments. Open circles, gray squares, and cross symbols are three strains originating from the eastern coast of Shikoku Island. The solid line represents an approximated function (n = 18, residual standard error = 0.041; see details in the "Materials and methods" section)

For sporophyte growth, we considered the DIN concentration and adopted the Michaelis-Menten function as follows:

$$f(N) = \mu_{max}\frac{N}{K_N + N} \tag{5}$$

where μ_{max} and K_N represent the maximum growth rate and the half saturation constant for DIN concentration, respectively. Laboratory experiments with young sporophytes have shown that the maximum relative growth rates are 0.262–0.285 day^{-1} (Murase et al. 2021), 0.258 day^{-1} (Morita et al. 2003), 0.20–0.25 day^{-1} (Gao et al. 2013), and 0.15–0.20 day^{-1} (Baba et al. 2006). In this study, we set μ_{max} to 0.25 day^{-1}. For young sporophytes, a nitrate concentration of ≥20 µgN L^{-1} (= 1.4 µM) is conducive to growth, as they wither at concentrations of <10 µgN L^{-1} (= 0.7 µM) (Kakehi et al. 2018; Kaga et al. 2022). Discoloration of sporophytes was observed at DIN concentrations below 2 µM in the Naruto area (Makino et al. 2015). Previous laboratory studies have shown that half saturation constants for nitrate and ammonium have wide ranges (2.2 and 407.2 µM, Torres et al. 2004; approximately 10–20 and 10–90 µM, Dean and Hurd 2007; 0.1–149 and 7.8–182 µM, Sato et al. 2016). K_N was estimated to be 17 µg N L^{-1} (= 1.2 µM) using the total nitrogen content in blades obtained from field observations (Kitadai and Kadowaki 2004). In this study, we adopted K_N as 1.2 µM based on these findings.

Water motion is a crucial factor for nutrient uptake in macroalgae (Hurd et al. 1996; Yoshida et al. 2011). Previous studies have indicated the effect of water flow velocity on the growth of *U. pinnatifida* sporophytes (Baba et al. 2006; Nanba et al. 2011). Following Hurd et al. (1996), the function of water current speed is expressed as an exponential formula:

$$f(U) = \left\{1 - \exp\left(\frac{-U}{U_c}\right)\right\} \tag{6}$$

where U_c represents the critical current speed at which the nutrient uptake rate is 63% of the maximum. Based on growth experiments of young sporophytes in an outdoor raceway tank system, which demonstrated relatively low growth rates in cases of less than 0.05 m s^{-1} (Baba et al. 2006), U_c was set to 0.05 m s^{-1}.

Cultivation density influences the biomass production and morphology of *U. pinnatifida*, and the growth and/or quality decrease with excessive density (Kitadai and Kadowaki 2004; Gao et al. 2014; Dan et al. 2015; Sato et al. 2023). In the Naruto area, thin seed ropes are cut to approximately 0.03 m and inserted into thick cultivation ropes at intervals of 0.3–0.5 m (Dan et al. 2015). This insertion interval was incorporated into the model as follows:

$$f(D) = \frac{D + \frac{D_s}{2}}{D + D_s} \tag{7}$$

where D_s represents the threshold value of the insertion interval. In this study, D_s was set to 0.5 m. The growth rate decreases with a decrease in the insertion interval of the seed rope D. If D is zero, the function becomes 0.5.

Several studies have explored the relationships between blade erosion for *U. pinnatifida* sporophytes and various factors such as water temperature (Stuart 1997), DIN concentration (Yoshikawa et al. 2001), and age (Nishikawa 1967). However, Dean and Hurd (2007) reported no significant correlation between erosion rates and any environmental property. In this study, we present an erosion function dependent on the TL of the sporophyte as follows:

$$f\left(L^2\right) = mL^{2\sigma} \tag{8}$$

where m represents the erosion rate and σ is a constant coefficient. We set σ to 0.5, indicating that the function value increases linearly with the TL. The value of m was diagnostically determined to be 0.06 m^{-1} day^{-1} in order to reproduce the temporal changes in the growth of sporophytes observed at two stations in the western SIS.

While several studies have highlighted the effect of irradiance on the growth of *U. pinnatifida* sporophytes (Kitadai and Kadowaki 2004; Baba 2008), we did not consider irradiance conditions for the current growth model. This is because we assumed that there would be no significant difference in the surface layer among the areas, both in the present and future. The integration of the model was carried out using an Euler-forward scheme with a time step of 1 hour.

Field observation data for input and validation of the growth model

Our model's performance was initially validated using field observation data obtained by Takenaka et al. (2021). They conducted field experiments on the growth of *U. pinnatifida* sporophytes (insertion interval of seed rope $D = 0.2$ m) at five stations, ranging from the southern Bungo Channel to northern Hiroshima Bay, to examine the influences of environmental gradients. In this study, we used oceanographic data and the TL of sporophytes at two stations, located in the northeastern Bungo Channel (Stn. A, 33.314°N, 132.471°E) and southern Hiroshima Bay (Stn. S, 33.937°N, 132.402°E), as input and validation data for the growth model. These locations were chosen due to negligible damage from herbivorous fishes. Daily water temperature and monthly DIN concentration at both stations were linearly interpolated over time and used as input variables for the growth model. Mean current speeds observed at the two stations (0.070 m s^{-1} at Stn. A and 0.064 m s^{-1} at Stn. S) were also factored into the growth simulations. At Stn. A, the initial size of the sporophyte was 0.15 m on 22 December 2015, and the simulation ran until 13 April 2016. At Stn. S, the initial size was 0.35 m on 5 January 2016, and the simulation ran until 20 April 2016.

Environmental data sets and simulations in the 1990s and 2090s

We conducted numerical simulations across the entire coastal area of the SIS for both the 1990s and the 2090s. To simulate the growth of the *U. pinnatifida* sporophyte we utilized environmental datasets comprising daily averaged water temperature, DIN concentration, and current speed in the surface layer. These datasets were generated by a coupled hydrodynamic-biogeochemical model with a horizontal resolution of 1 km, serving as input data for the growth model. The hydrodynamic-biogeochemical model incorporates benthic and pelagic systems, including the carbon–nitrogen–phosphorus-oxygen-coupled cycle (Higashi et al. 2020). The hydrodynamic model is based on the three-dimensional hydrostatic Boussinesq equations, solved by the finite difference method using a horizontal collocated and vertical z-level grid (Higashi et al. 2015). The biogeochemical model has compartments of phytoplankton (two diatoms and dinoflagellate), inorganic matter (ammonium, nitrate, phosphate, and adsorbed phosphorus), particulate organic matter (fast- and slow-labile), dissolved organic matter (fast- and slow-labile), and dissolved oxygen. For the simulations, the model was driven by 1 present (PRSNT: HPA_m02) and 4 future cases (RCP2.6: HFA_rcp26_c3, RCP4.5: HFA_rcp45_c3, RCP6.0: HFA_rcp_c3, RCP8.5: HFA_rcp_c3) of atmospheric conditions among 19 ensemble cases obtained from the Non-Hydrostatic Regional Climate Model (NHRCM; Sasaki et al. 2008) with 20 km horizontal resolution. Boundary conditions and input data for present climate simulation were sourced from a four-dimensional variational ocean reanalysis for the Western North Pacific over 30 years (FORA-WNP30; Usui et al. 2017). Future conditions were adjusted by incorporating the change in linear trend predicted by the Model for Interdisciplinary Research on Climate version 5 (MIROC5; Watanabe et al. 2010). Terrestrial nutrient loads and nutrient concentrations at the lateral ocean boundaries remained consistent across present and future climate cases, with the former being based on numerical simulations of water pollutant emissions in 2014 surveyed by the Japan Ministry of Environment, and the latter being climatological data from the World Ocean Atlas 2009 (Garcia et al. 2010). The hydrodynamic-biogeochemical model effectively replicated physical conditions and water qualities in the SIS at the end of the 20th century and projected them for the end of the 21st century under four emission scenarios (RCP2.6, 4.5, 6.0, and 8.5). Detailed information regarding model configuration and performance can be found in Higashi et al. (2019; 2020; 2018). These studies accurately estimated and incorporated the terrestrial discharges of freshwater and nutrients, and carefully validated the spatio-temporal dynamics of simulated water temperature, salinity, chlorophyll-*a* concentration estimated from phytoplankton, and total nitrogen concentration using observed data. The datasets simulated by the hydrodynamic-biogeochemical model are available via the website of the National Institute for Environmental Studies, Japan (Higashi 2022). Additionally, the M_2 tidal current amplitude calculated by the two-dimensional tidal model (Guo et al. 2013) was incorporated into the daily averaged current speed in each grid. This adjustment was necessary as the daily averaged current speed did not encompass the semi-diurnal tidal currents predominant in the SIS. The tidal model had the same horizontal resolution (i.e., 1 km) as the hydrodynamic-biogeochemical model and nearly the same model domain. Given that most cultivations are restricted to nearshore areas, we utilized environmental data within one grid from the shore for the growth model. The cultivation season for *U. pinnatifida* sporophyte spanned from autumn in one year to the following spring (i.e., the cultivation season in 1990 ranged from autumn 1990 to spring 1991). Simulations for the 1990s and the 2090s were conducted by calculations covering the cultivation seasons from 1990 to 1999 and from 2090 to 2099, respectively.

In the cultivation process, juvenile sporophytes attached to seed ropes are transferred to the ambient sea area for nursery cultivation once the water temperature drops below 23℃. Nursery cultivation typically lasts from approximately three weeks to one month, allowing the juveniles to grow to one or a few centimeters (Dan et al. 2015; Tanada et al. 2015; Niwa 2016; Niwa and

Kobiyama 2019; Yoshida et al. 2019). Following these schedules, the growth model simulations were initiated 20 days after the water temperature fell below 23℃ in each grid. The initial size of the sporophyte and the insertion interval of the seed rope *D* were set to 0.01 m and 0.4 m, respectively. All simulations for both the 1990s and the 2090s under climate change scenarios were carried out until 30 April each year.

On a different note, new cultivars with high-temperature tolerance have been developed through crossbreeding in recent years as part of climate change adaptation strategies (Tanada 2016; Niwa and Kobiyama 2019; Murase et al. 2021). Niwa and Kobiyama (2019) observed significant growth in many young sporophytes of the new cultivar during nursery cultivation, despite the early start at a high temperature of 24.5℃. Similarly, Murase et al. (2021) found that the new cultivar with high-temperature tolerance exhibited the same optimal temperature range for growth (15℃–20℃) as the conventional cultivar, yet demonstrated a high survival rate even at temperatures of ≥25℃. In addition to the previous simulations, we conducted another simulation focusing on climate change adaptation in the 2090s. Assuming that the new cultivar could thrive under early start timing (i.e., high water temperature conditions) for nursery and subsequent full cultivation, the adaptation simulation commenced 20 days after the water temperature dropped below 25℃, while maintaining the same other conditions.

Results

Model validation using field observation data

Temporal variations in water temperature, DIN concentration, and TL of sporophyte at two stations used for model validation are depicted in Fig. 3. Throughout the observation period, the water temperature and DIN concentration at Stn. A consistently exceeded those at Stn. S. At Stn. A, water temperature and DIN concentration were 13.4–18.0℃ and 2.5–10.6 μM, respectively. Meanwhile, at Stn. S, water temperature and DIN concentration were 10.9–14.6℃ and 0.1–5.1 μM, respectively. The TL of sporophyte at Stn. A, exhibited rapid growth from 0.15 m in late December 2015 to 1.20 m in early March 2016, followed by a decline to 0.75 m in mid-April 2016. Conversely, the growth rate at Stn. S remained relatively low, with the maximum TL reaching 0.64 m in late March 2016. The simulation outcomes at both stations accurately replicated the observed temporal changes in TL of the sporophyte, except for the deviation observed at Stn. A in April 2016.

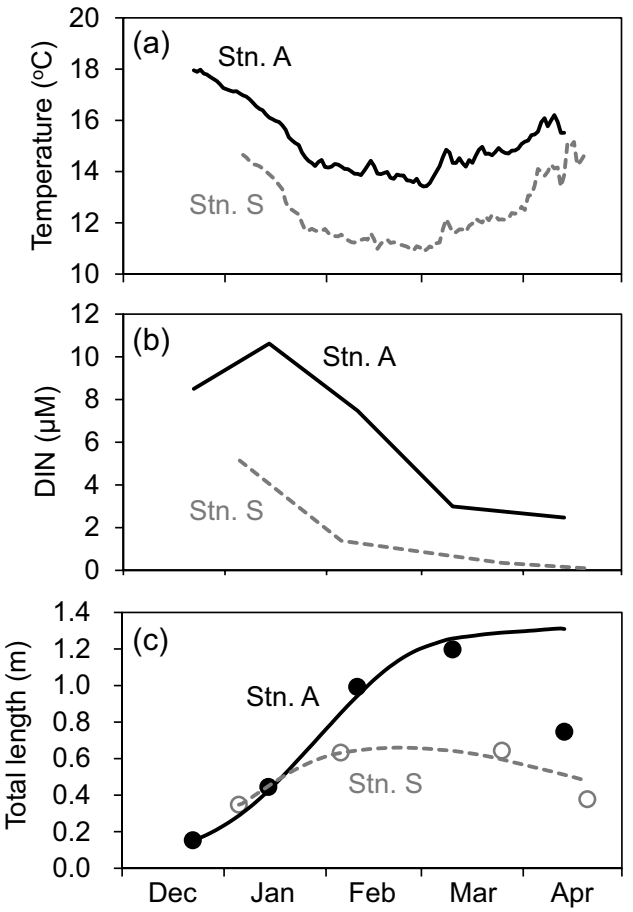

Fig. 3 Temporal changes in (**a**) water temperature and (**b**) DIN concentration observed at Stns. A and S (solid black and broken gray lines), alongside (**c**) the total length of *Undaria pinnatifida* sporophyte observed (closed black and open gray circles) and simulated (solid black and broken gray lines) at Stns. A and S

Simulations in the 1990s and 2090s

Environmental conditions

Temporal variations in water temperature, DIN concentration, and current speed from November to April, averaged over the simulation area encompassing the entire SIS, are presented in Fig. S1. Both water temperature and DIN concentration exhibited distinct seasonal variations in both the 1990s and the 2090s. Specifically, water temperature reached its minimum in February-March, while DIN concentration peaked in December-January. Notably, water temperature showed an overall increase, and DIN concentration exhibited a general decrease in the 2090s, particularly under higher RCP scenarios. The average water temperature from November to March was 14.7℃ in the 1990s, compared to 15.7°C, 16.4°C, 16.9℃, and 18.2℃ in the 2090s under the RCP2.6, 4.5, 6.0, and 8.5 scenarios, respectively. The difference in water temperature between the 1990s and the 2090s under

the RCP8.5 scenario was approximately 3.5°C. In contrast, current speed exhibited slight seasonal variation with peaks in January-February, and this pattern remained consistent between the 1990s and the 2090s across all RCP scenarios.

Fig. S2 illustrates the distributions of surface water temperature, DIN concentration, and current speed averaged from November to March in the 1990s and the 2090s. These variables displayed significant geographical contrasts among different areas in both time periods. The water temperature was relatively high in the Bungo and Kii Channels, which connect to the Pacific Ocean, while it was lower in Suo-Nada, a shallow basin, and Bisan-Seto, a narrow channel. Although water temperature increased in the 2090s under higher RCP scenarios, the differences in increasing rates among different areas were not substantial. High DIN concentrations (>5 μM) were observed at major river mouths and in the inner part of Osaka Bay, while relatively low DIN concentrations were found in Hiuchi-Nada, Aki-Nada, and southern Hiroshima Bay, both in the 1990s and the 2090s. Large current speeds (>0.5 m s^{-1}) were predominantly distributed in areas surrounding the straits and narrow channels with numerous small islands, consistent across both time periods.

Fig. S3 illustrates the spatial distributions of the first days below 23℃ and 25℃, which serve as criteria for the initiation of current cultivation and cultivation of a high-temperature tolerant cultivar, respectively. In the 1990s, the first day below 23℃ occurred between early October and early November. This onset was earlier around the Bungo Channel and along the coast of Honshu. However, in the 2090s, this day was progressively delayed with higher RCP scenarios. The average onset across all coastal grids in Fig. S3, encompassing the SIS and the Pacific Ocean, shifted from 18 October in the 1990s to 21 November in the 2090s under the RCP8.5 scenario. In certain areas, particularly under the RCP8.5 scenario, the first day below 23℃ was delayed until December in 2090. This delay was more pronounced in the western SIS regions such as the Bungo Channel, Iyo-Nada, and Aki-Nada, but less so in Bisan-Seto. Similarly, the spatial distribution of the first day below 25℃ mirrored that of the first day below 23℃ in each scenario, albeit occurring earlier. Under the RCP2.6 scenario, this onset was notably earlier than in the 1990s. The average onset across all coastal grid points under the RCP8.5 scenario was nearly identical to the onset below 23℃ under the RCP4.5 scenario.

Growth dynamics of sporophyte in the Naruto area

In the Naruto area the primary cultivation zone in the SIS, we compared the growth dynamics of sporophytes between the 1990s and the 2090s (Fig. 4). During the 1990s full cultivation typically commenced on 14 November averaged over the Naruto area for a decade. The TL of sporophytes reached approximately 1 m by late February, surpassing 1.4 m in early April. However, in the 2090s, the initiation of cultivation was consistently delayed across all RCP scenarios due to ocean warming. The mean start dates were postponed by 9 days compared to the 1990s under the RCP2.6 scenario, by 14 days under the RCP4.5 scenario, by 21 days under the RCP6.0 scenario, and by 30 days under the RCP8.5 scenario, respectively. While the growth curve under the RCP2.6 scenario trailed behind that of the 1990s until the end of February, sporophyte size exceeded the 1990s levels in March. Conversely, the growth curves under the RCP4.5, 6.0, and 8.5 scenarios remained below the 1990s levels throughout the cultivation season. By the end of March, the mean TL ratios to the 1990s were 104%, 88%, 86%, and 77% under the RCP2.6, 4.5, 6.0 and 8.5 scenarios, respectively. Sporophyte growth decelerated in April, with mean TL at the end of April remaining consistent with end-of-March levels in both the 1990s and the 2090s, irrespective of RCP scenarios.

In simulations conducted in the 2090s for climate change adaptation using a high-temperature tolerant cultivar (RCP2.6, 4.5, 6.0 and 8.5 adpt), the mean start dates were advanced by 9 days compared with the 1990s under the RCP2.6 scenario, and the dates were postponed by 3, 4 and 15 days compared with the 1990s under the RCP4.5, RCP6.0 and RCP8.5 scenarios, respectively. Under the RCP2.6 scenario, the mean TL of sporophytes exceeded the 1990s levels throughout the cultivation season. The growth curves under the RCP4.5 and 6.0 scenarios exhibited temporal changes quite similar to those in the 1990s, with the difference between the 2090s under the RCP8.5 scenario and the 1990s diminishing compared to the non-adaptation case. At the end of March, the mean TL ratios to the 1990s were 112%, 98%, 97%, and 92% under the RCP2.6, 4.5, 6.0, and 8.5 scenarios, respectively. In April, the TL of sporophytes either remained at the same level or began to decline across all RCP scenarios.

Spatial distributions of sporophyte growth

There were notable geographical variations in sporophyte growth among different areas during the 1990s (Fig. 5). At the end of March, large TLs of sporophytes >1.4 m were seen in regions such as the Bungo and Kii Channels, as well as in the eastern SIS encompassing Osaka Bay, Harima-Nada, and Bisan-Seto. Conversely, relatively smaller TLs below 1.0 m were noted in the western-central SIS areas, including Suo-Nada, Hiroshima Bay, Hiuchi-Nada, and along the Pacific coast.

In the 2090s, while TLs under the RCP2.6 scenario exhibited a partial increase of up to 10% in the eastern SIS compared to the 1990s, TLs under the RCP4.5, 6.0, and 8.5 scenarios decreased in most regions, except for the large river mouths and the inner part of Osaka Bay (Fig. 6). Particularly

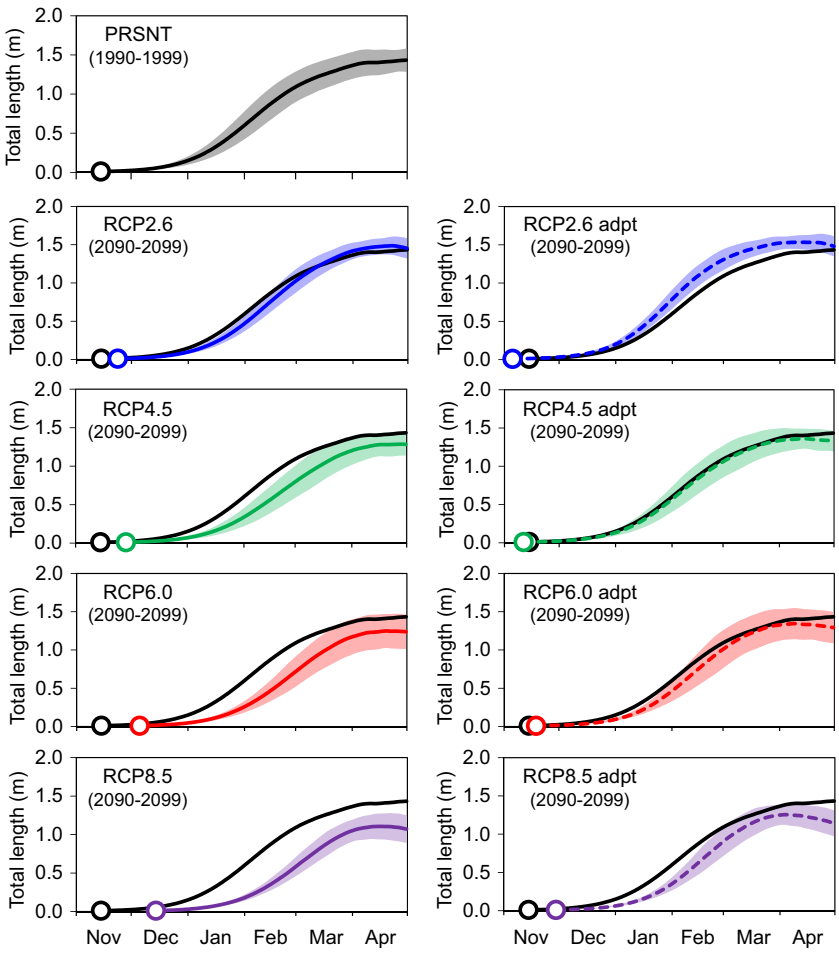

Fig. 4 Temporal changes in the total length of *Undaria pinnatifida* sporophyte in the Naruto area (the rectangle area in the lower panel of Fig. 1) during the 1990s under present climate conditions (PRSNT) and the 2090s under future climate conditions based on the RCP2.6, 4.5, 6.0, and 8.5 scenarios. The cases for climate change adaptation using a high-temperature-tolerant cultivar are depicted in the right four figures (RCP2.6, 4.5, 6.0, and 8.5 adpt). Open circles indicate the median start days of cultivation among 10 years, averaged over the Naruto area. Solid lines and colored areas represent the means and standard deviations for 10 years. The start day of cultivation and the mean total length of sporophyte in the 1990s are overlaid in the 2090s

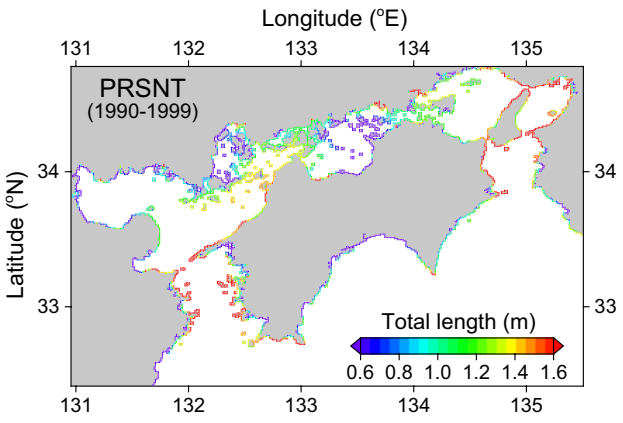

Fig. 5 Distribution of the total length of *Undaria pinnatifida* sporophyte on 31 March, averaged over the 1990s

noteworthy was the decrease rate of >40% observed in the Bungo Channel and the western SIS areas like Iyo-Nada, Hiroshima Bay, and Aki-Nada under the RCP8.5 scenario. In cases involving climate change adaptation, TLs increased across all areas compared to cases without adaptation in the 2090s. Under the RCP2.6 scenario with adaptation, TLs in the 2090s surpassed those of the 1990s in nearly all areas of the SIS, with the highest increase observed in the eastern SIS, especially in Bisan-Seto. Even under the RCP4.5, 6.0, and 8.5 scenarios, TLs in the eastern SIS were larger than those observed in the 1990s.

Sensitivity analyses

We conducted sensitivity analyses to assess the impact of individual environmental factors under climate change scenarios on sporophyte growth. In these analyses, we simulated sporophyte growth considering three environmental factors (water temperature, DIN concentration, and current speed) individually in the 2090s compared to the conditions in the 1990s (Fig. 7). In cases where only water temperature changed, sporophyte growth increased in Suo-Nada and Bisan-Seto, where water temperatures were relatively low during winter, but decreased in Iyo-Nada, Hiroshima Bay, Aki-Nada, Hiuchi-Nada, and along the Pacific coast. These geographical contrasts were more pronounced in higher RCP scenarios. Conversely, in cases where only DIN concentration changed, TL gradually decreased in almost all areas, particularly with higher RCP scenarios. Changes in current

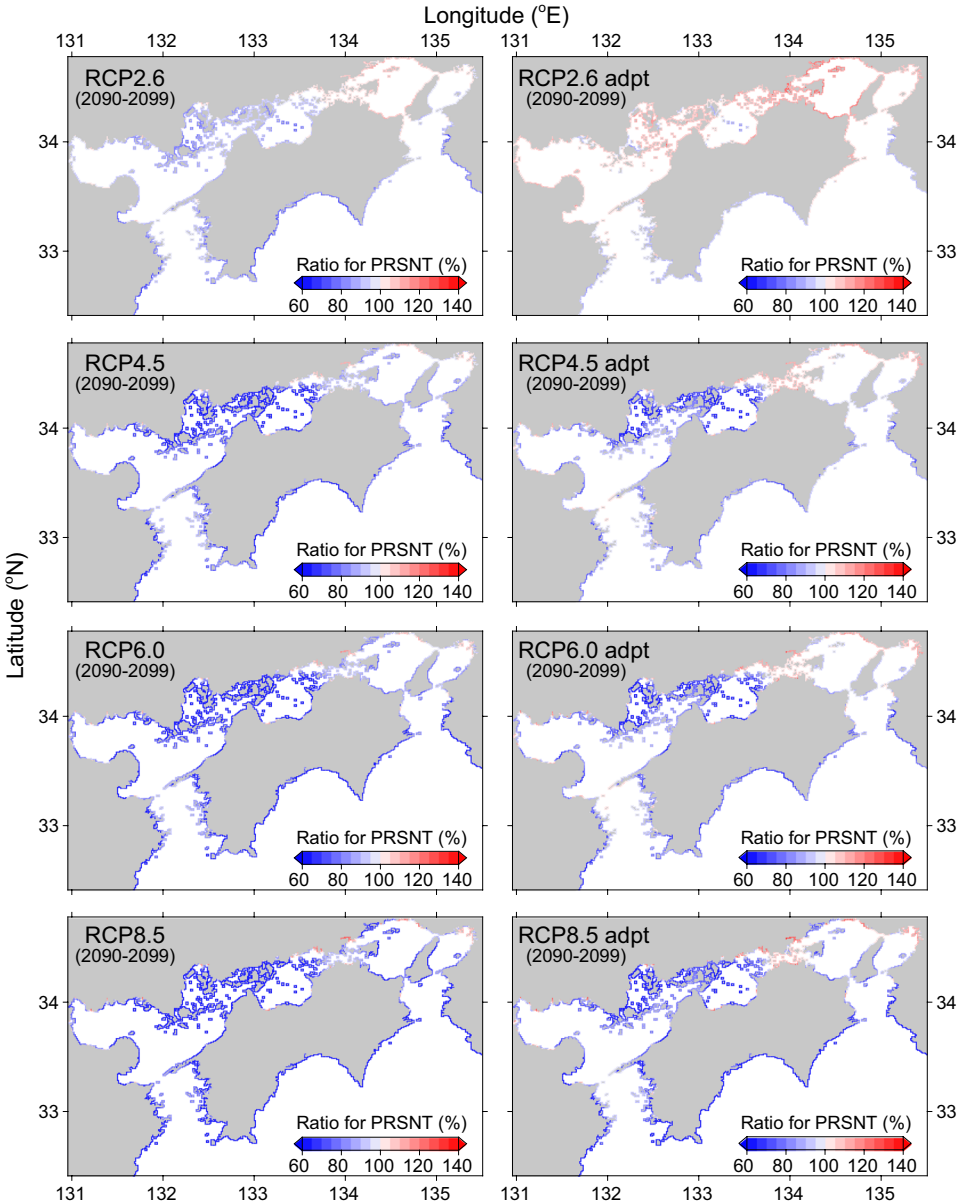

Fig. 6 Distribution of the ratios of the total length of *Undaria pinnatifida* sporophyte in the 2090s under the RCP2.6, 4.5, 6.0, and 8.5 scenarios, compared to the 1990s. The four figures on the right show the cases for climate change adaptation

speed had minimal effects on the growth of *U. pinnatifida* sporophytes.

Discussion

To assess the potential impacts of future climate change scenarios on the cultivation of *U. pinnatifida*, we developed an individual-based growth model for its sporophyte. Initially, we validated the model's performance using field observation data (Fig. 3). The water temperature at Stn. A was found to be more conducive to growth, as the average temperature over the cultivation period were closer the T_{opt} compared to that at Stn. S. Similarly, DIN concentration at Stn. A appeared more advantageous for growth compared to Stn. S. Our simulation results replicated the temporal changes in TL of sporophytes at these two stations, despite their differing oceanographic conditions. In the subsequent step, we conducted numerical simulations for both the 1990s and the 2090s under various RCP scenarios to assess the impacts of climate change on sporophyte growth, both in the Naruto area and across the entire SIS.

In the Naruto area, the simulated growth curve of the sporophyte in the 1990s (Fig. 4) closely aligned with observations from previous studies (Dan and Kato 2008; Kato and Dan 2010; Tanada et al. 2015; Niwa and Kobiyama 2019). TL in the 2090s, except for the RCP2.6 scenario, exhibited relatively lower values than the 1990s because of the delayed initiation time of cultivation (Fig. S3) and a decrease in DIN concentration (Fig. S2). The simulated TLs in the 2090s

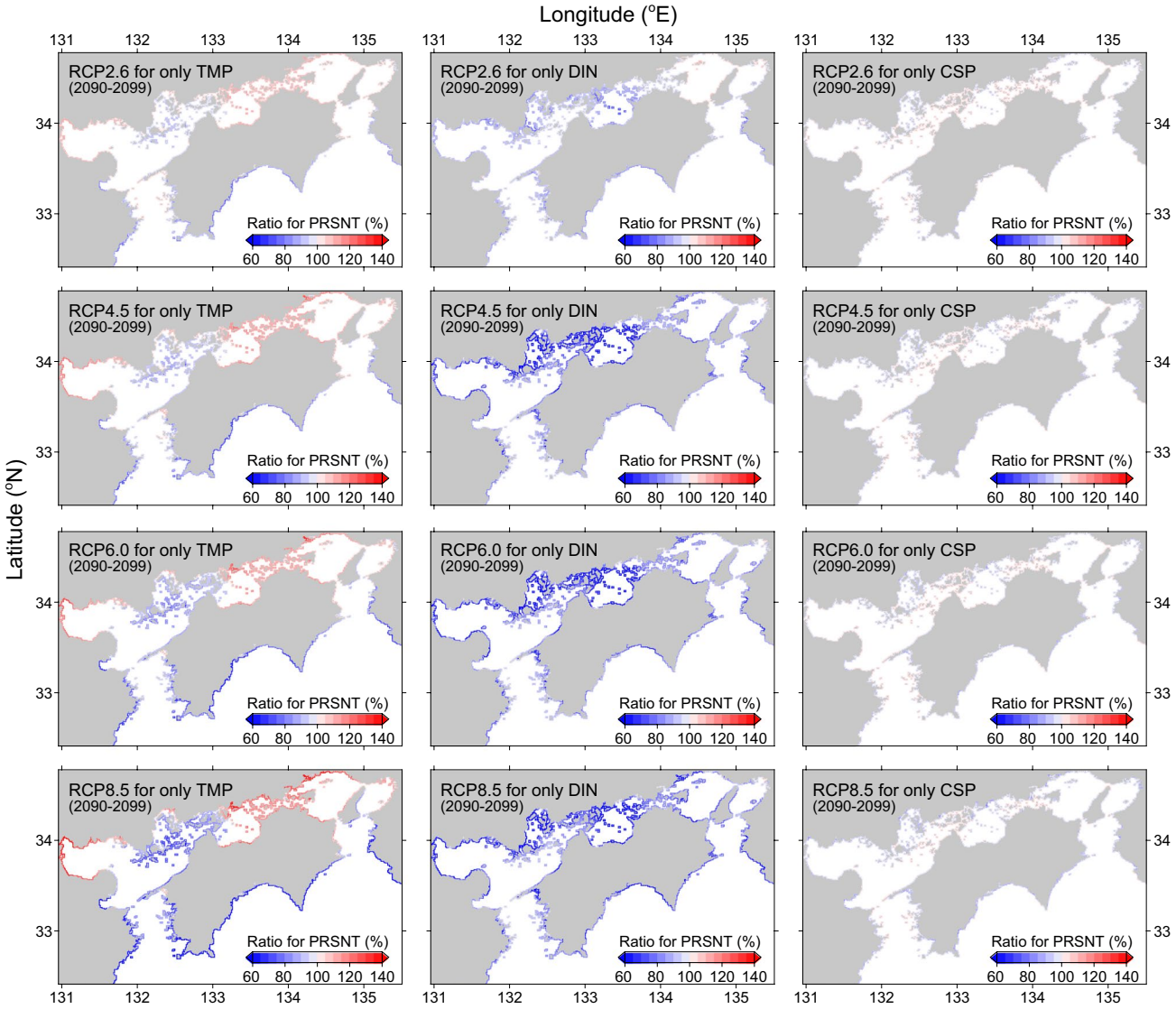

Fig. 7 Similar to Fig. 6, but under the RCP2.6, 4.5, 6.0, and 8.5 scenarios, considering only changes in water temperature, DIN concentration, and current speed

under the RCP4.5, 6.0, and 8.5 scenarios indicated decreases of 12–23% at the end of March. The exponential relationship between TL and wet weight (e.g., Kato and Nakahisa 1962; Yoshikawa et al. 2001) implies significant yield losses in the 2090s. Nevertheless, the growth rate in February-March was higher in the 2090s compared to the 1990s because the water temperature during that period approached the optimum temperature for growth (17.37℃, T_{opt} in Eq. 4) due to the increase in water temperature. In the case of the RCP2.6 scenario, the mean TL exceeded 100% of the 1990s at the end of March, suggesting the potential for increased yield in the 2090s. On the other hand, simulations for climate change adaptation using a new cultivar with high-temperature tolerance projected a suppression of TL decrease. The TL with a high-temperature tolerant cultivar decreased only 8% at the end of March in the 2090s even under the RCP 8.5 scenario, while the conventional cultivar decreased 23% (Fig. 4). Given that cultivations of high-temperature tolerant cultivars could commence earlier, it may be possible to mitigate yield loss. Alternatively, adjusting the end of cultivation to maintain a consistent cultivation period is another option, but our study suggests that this may not result in increased yields as sporophyte growth slows down in April. Overall, the simulation results underscore the significant impacts of ocean warming on *U. pinnatifida* cultivation and highlight the effectiveness of climate change adaptation through the use of a high-temperature tolerant cultivar in the Naruto area. Technological developments, such as onshore nursery cultivation, to accelerate the start timing of cultivation are anticipated to help sustain cultivation yields.

The spatial distribution of TL in the 1990s indicates higher sporophyte growth in the eastern SIS (Fig. 5), aligning with actual cultivation areas (https://www.jfa.maff.go.jp/j/enoki/gyogyouken_jouhou3.html); accessed 8 December 2023 and suggesting potential for future expansion of aquaculture scale, particularly in areas like the northern part of Osaka Bay where cultivation is currently not conducted. In the eastern SIS, although the average water temperature is relatively low, DIN concentration is comparatively high compared to other areas (Fig. S2), and current speeds are elevated in the Naruto area and other strait areas (Fig. S2), making these oceanographic conditions conducive to growth. Additionally, high growth in the Bungo Channel is observed, attributed to the criterion of 23℃ at the start of cultivation (Fig. S3). Intermittent decreases in water temperature due to bottom cold-water intrusion from the continental shelf slope (Kaneda et al. 2002) and tidal mixing (Nagai and Hibiya 2012) around the Bungo Channel during stratified seasons contribute to a relatively extended cultivation period with an early start timing, resulting in large TL in the area.

As highlighted, the increase in water temperature has both negative and positive effects on *U. pinnatifida* cultivation. While it delays the start of cultivation, it also accelerates sporophyte growth by approaching the optimum temperature for growth. Sensitivity analysis focusing on changing water temperature (Fig. 7) indicates enhanced sporophyte growth in Suo-Nada, Bisan-Seto, and Harima-Nada, where winter water temperatures (Fig. S2) are significantly lower than the optimum. This is consistent with the higher growth rate in the Naruto area during the 2090s compared with the 1990s from February to March, as depicted in the simulated time series. Conversely, in areas like the Bungo Channel, Iyo-Nada, and the eastern Kii Channel, where winter water temperatures are closer to the optimum, the positive effect is relatively minor. The sensitivity analyses suggest that the ratio of positive/negative impacts will lead to enhanced geographical contrasts of sporophyte growth in the SIS with higher RCP scenarios. Notably, Bisan-Seto appears to hold potential for future growth promotion in cultivation. Given the documented long-term increase in water temperature in the SIS over recent decades (Nishikawa et al. 2010; Abo et al. 2018), continuous monitoring of future trends in water temperature and their effects on *U. pinnatifida* cultivation is essential.

DIN concentrations in the 2090s under all RCP scenarios were lower than those in the 1990s in the SIS. Since the decrease in nutrient concentration directly influences the growth of *U. pinnatifida* sporophyte, the sensitivity analysis focusing solely on changing DIN concentration revealed a decrease in TL in almost all areas in the 2090s (Fig. 7). Consequently, TLs in the 2090s under the RCP4.5, 6.0, and 8.5 scenarios decreased even in areas where an increase in TL would have been predicted solely by increasing water temperature. In our simulation, DIN concentration was calculated assuming that current nutrient loads would remain unchanged in the 2090s. The decrease in DIN concentration, despite the assumption of unchanged nutrient loads, is attributed to increased phytoplankton consumption due to higher water temperatures in winter (Higashi et al. 2020). The SIS became eutrophic in the 1960s and 1970s due to anthropogenic nutrient loads, but subsequent measures to reduce nutrient loads have led to a significant decrease in nutrient concentrations (Yamamoto 2003; Yanagi 2015). In recent years, the impact of nutrient deficiency on fisheries production has been indicated, leading to legislative changes moving toward nutrient management (Abo and Yamamoto 2019). Terrestrial anthropogenic nutrient loads depend on demographic and social conditions and affect nutrient concentrations, particularly in the nearshore area of the SIS (Abo et al. 2018; Leng et al. 2023). Therefore, it is important to note that the simulation results include uncertainty regarding DIN concentration in the 2090s. In recent years, countermeasures such as the utilization of fertilizer in farming areas have been developed in preparation for the decrease in ambient nutrients (Ikewaki et al. 2016).

In this study, it should be noted that the risk of herbivory was not considered in the simulations. Previous research has documented feeding damages inflicted on *U. pinnatifida* by herbivorous fishes and isopods through field and laboratory experiments (Yamaguchi 2010; Tanada et al. 2019; Endo et al. 2021; Noda and Murase 2021; 2022; Takenaka et al. 2021). Typically, feeding damage occurs during warmer periods, particularly above 15℃–20°C, and is less likely during colder winter months when temperatures drop below 15°C (Yamaguchi 2010; Endo et al. 2021; Takenaka et al. 2021). By not accounting for feeding damage, this study may underestimate the impact of reduced production attributed to ocean warming in future projections. Although high-temperature tolerant cultivars are expected to be developed, addressing feeding damage remains a crucial consideration for climate change adaptation. Strategies such as the development of repellents and guards against herbivorous fish have been explored (Hori et al. unpublished data). Additionally, the application of blue light emission to young sporophytes has shown promise in boosting *U. pinnatifida* production by promoting growth and deterring grazers (Suzuki et al. 2019). These technological advancements should be integrated with the introduction of new cultivars with high-temperature tolerance to ensure the sustainability of the aquaculture industry.

Seaweed farming is anticipated to contribute to climate change mitigation and adaptation due to its dual role as a carbon sink and food source (Duarte et al. 2017; Spillias et al. 2023). As such, the need for quantitative evaluation of seaweed farming is expected to increase steadily. In this study, we developed and applied an individual-based growth

model that explicitly describes the physiological processes of the *U. pinnatifida* sporophyte. This model enables a quantitative assessment of the positive and negative effects of each environmental factor on seasonal sporophyte growth. While the TL of the sporophyte was used as the objective variable in this study, for evaluating yields in the area, quantitative estimates of biomass (weight) will be needed. This includes not just single sporophyte growth but also community biomass, such as weight per unit length of rope. Such quantitative estimates are essential for feasibility and sustainability of aquaculture farming. Furthermore, it is also possible to elucidate the material cycle and estimate the resulting carbon uptake by considering the contents of biophile elements such as C, N, and P. Previous studies have already developed an individual-based growth model that includes nitrogen and carbon reserves. The model is coupled with a 3D hydrodynamic-biogeochemical model and has been used to evaluate the cultivation potential of sugar kelp, *Saccharina latissima*, in Norway (Broch et al. 2013; 2019). The further development of the present model of *U. pinnatifida* sporophyte will be the focus of future work.

Supplementary Information The online version contains supplementary material available at https://doi.org/10.1007/s10811-024-03291-1.

Acknowledgments We thank Drs. Norio Tanada, Masakazu Hori, and Hideaki Kidokoro for helpful and constructive comments.

Authors' contributions G. Onitsuka: Designing the research, developing and simulating the sporophyte growth model, writing the original draft and editing the manuscript. G. Yoshida: Designing the research, conducting the field experiments, reviewing and editing the manuscript. H. Shimabukuro, S. Takenaka, T. Tamura: Conducting the field experiments, reviewing and editing the manuscript. S. Kakehi: Developing the sporophyte growth model, reviewing and editing the manuscript. T. Setou, X. Guo, H. Higashi: Preparing the environmental data set obtained from the hydrodynamic-biogeochemical model and the tidal model, reviewing and editing the manuscript. All authors approved the manuscript for submission.

Funding This study was supported by the Environment Research and Technology Development Fund (JPMEERF20S11809) of the Environmental Restoration and Conservation Agency of Japan.

Data availability The datasets generated during and/or analyzed during the current study are available from the corresponding author on reasonable request.

Declarations

Competing interests The authors declare that they have no conflict interests.

References

Abo K, Yamamoto T (2019) Oligotrophication and its measures in the Seto Inland Sea, Japan. Bull Jpn Fish Res Edu Agen 49:21–26

Abo K, Akiyama S, Harada K, Nakaji Y, Hayashi H, Murata K, Wanishi A, Ishikawa Y, Masui T, Nishikawa S, Yamada K, Noda M, Tokumitsu S (2018) Long-term variations in water quality and causal factors in the Seto Inland Sea, Japan. Bull Coast Oceanogr 55:101–111 (in Japanese with English abstract)

Baba M (2008) Effects of temperature, irradiance and salinity on the growth of *Undaria pinnatifida* from Niigata Prefecture, Central Japan. Rep Mar Ecol Res Inst 11:7–15 (in Japanese with English abstract

Baba M, Yamamoto M, Watanabe Y (2006) Growth responses to water temperature and water velocity of *Undaria pinnatifida* (Phaeophyceae) under outdoor raceway tank system. Rep Mar Ecol Res Inst 9:55–64 (in Japanese with English abstract)

Broch OJ, Slagstad D (2012) Modelling seasonal growth and composition of the kelp *Saccharina latissima*. J Appl Phycol 24:759–776

Broch OJ, Ellingsen IH, Forbord S, Wang X, Volent Z, Alver MO, Handå A, Andresen K, Slagstad D, Reitan KI, Olsen Y, Skjermo J (2013) Modelling the cultivation and bioremediation potential of the kelp *Saccharina latissima* in close proximity to an exposed salmon farm in Norway. Aquacult Environ Interact 4:187–206

Broch OJ, Alver MO, Bekkby T, Gundersen H, Forbord S, Handå A, Skjermo J, Hancke K (2019) The kelp cultivation potential in coastal and offshore regions of Norway. Front Mar Sci 5:529

Chang PH, Guo X, Takeoka H (2009) A numerical study of the seasonal circulation in the Seto Inland Sea, Japan. J Oceanogr 65:721–736

Dan A, Kato S (2008) Differences of morphology and growth between the two culture varieties originating from *Undaria pinnatifida* f. *distans* and *U. pinnatifida* f. *typica* in Naruto Strait. Bull Tokushima Pref Fish Res Ins 6:79–83 (in Japanese withEnglish abstract)

Dan A, Ohno M, Matsuoka M (2015) Changes of the research and development on the resources of *Undaria* and *Laminaria* in the culture ground of Tokushima coasts. Bull Tokushima Pref Fish Res Ins 10:25–48 (in Japanese)

Dean PR, Hurd CL (2007) Seasonal growth, erosion rates, and nitrogen and photosynthetic ecophysiology of *Undaria pinnatifida* (Heterokontophyta) in southern New Zealand. J Phycol 43:1138–1148

Duarte CM, Wu J, Xiao X, Bruhn A, Krause-Jensen D (2017) Can seaweed farming play a role in climate change mitigation and adaptation? Front Mar Sci 4:100

Endo H, Okumura Y, Sato Y, Agatsuma Y (2017) Interactive effects of nutrient availability, temperature, and irradiance on photosynthetic pigments and color of the brown alga *Undaria pinnatifida*. J Appl Phycol 29:1683–1693

Endo H, Sato Y, Kaneko K, Takahashi D, Nagasawa K, Okumura Y, Agatsuma Y (2021) Ocean warming combined with nutrient enrichment increases the risk of herbivory during cultivation of the marine macroalga *Undaria pinnatifida*. ICES J Mar Sci 78:402–409

Epstein G, Smale DA (2017) *Undaria pinnatifida*: A case study to highlight challenges in marine invasion ecology and management. Ecol Evol 7:8624–8642

FAO (2022) The State of World Fisheries and Aquaculture 2022. Towards Blue Transformation. FAO, Rome. https://doi.org/10.4060/cc0461en. Accessed 8 Dec 2023

FAO, WHO (2022) Report of the expert meeting on food security for seaweed-Current status and future perspectives. Rome, 28–29 October 2021. Food Safety and Quality Series No. 13, FAO and WHO, Rome. https://doi.org/10.4060/cc0846en. Accessed 8 Dec 2023

Froehlich HE, Afflerbach JC, Frazier M, Halpern BS (2019) Blue growth potential to mitigate climate change through seaweed offsetting. Curr Biol 29:3087–3093

Gao X, Endo H, Taniguchi K, Agatsuma Y (2013) Combined effects of seawater temperature and nutrient condition on growth and survival of juvenile sporophytes of the kelp *Undaria pinnatifida*

(Laminariales; Phaeophyta) cultivated in northern Honshu, Japan. J Appl Phycol 25:269–275
Gao X, Endo H, Taniguchi K, Agatsuma Y (2014) Effects of experimental thinning on the growth and maturation of the brown alga *Undaria pinnatifida* (Laminariales; Phaeophyta) cultivated in Matsushima Bay, northern Japan. J Appl Phycol 26:529–535
Garcia HE, Locarnini RA, Boyer TP, Antonov JI, Zweng MM, Baranova OK, Johnson DR (2010) World Ocean Atlas 2009, Volume 4: Nutrients (phosphate, nitrate, silicate). In: Levitus S (ed) NOAA Atlas NESDIS 71. US Government Printing Office, Washington DC, p 398
Guo X, Harai K, Kaneda A, Takeoka H (2013) Simulation of tidal currents and nonlinear tidal interactions in the Seto Inland Sea, Japan. Rep Res Inst Appl Mech Kyushu Univ 145:43–52
Higashi H, Morino Y, Furuichi N, Ohara T (2015) Ocean dynamic processes causing spatially heterogeneous distribution of sedimentary caesium-137 massively released from the Fukushima Daiichi Nuclear Power Plant. Biogeosciences 12:7107–7128
Higashi H, Sato Y, Yoshinari H, Maki H, Koshikawa H, Kanaya G, Uchiyama Y (2018) Freshwater discharge from small river basins and its impacts on reproducibility of coastal hydrodynamic simulation in Seto Inland Sea. J Jpn Soc Civ Eng B2:I_1135-I_1140 (in Japanese with English abstract)
Higashi H, Akiyama C, Nakada S, Yoshinari H (2019) A distributed river runoff model for Seto Inland Sea basin and trend in total nitrogen loading for the decade 2006–2015. J Jpn Soc Civ Eng B1:I_421-I_426 (in Japanese with English abstract)
Higashi H, Yokoyama A, Nakada S, Yoshinari H, Koshikawa H (2020) Climate change impacts on primary production and water quality in the Seto Inland Sea under RCP8.5 scenario. J Jpn Soc Civ Eng B2:I_1147-I_1152 (in Japanese with English abstract)
Higashi H (2022) Prediction dataset of climate change impact on water environment in the Seto Inland Sea, ver2021. NIES. https://doi.org/10.17595/20240119.001. Accessed 23 Feb 2024
Hurd CL, Harrison PJ, Druehl LD (1996) Effect of seawater velocity on inorganic nitrogen uptake by morphologically distinct forms of *Macrocystis integrifolia* from wave-sheltered and exposed sites. Mar Biol 126:205–214
Ikewaki Y, Makino K, Nishioka T, Hirano T, Ueta Y (2016) Development of fertilizer congealed with gelatin for seaweed culture. Nippon Suisan Gakk 82:917–922 (in Japanese with English abstract)
IPCC (2022) Climate Change 2022: Impacts, Adaptation and Vulnerability. Contribution of Working Group II to the Sixth Assessment Report of the Intergovernmental Panel on Climate Change In: Pörtner HO, Roberts DC, Tignor M, Poloczanska ES, Mintenbeck K, Alegría A, Craig M, Langsdorf S, Löschke S, Möller V, Okem A, Rama B (eds) Cambridge University Press, Cambridge. 3056
James K, Kibele J, Shears NT (2015) Using satellite-derived sea surface temperature to predict the potential global range and phenology of the invasive kelp*Undaria pinnatifida*. Biol Inv 17:3393–3408
Kaga S, Kakehi S, Naiki K, Kodama T, Wagawa T, Segawa S, Watanabe S, Musashi T, Kuroda H, Ito SI (2022) Seasonal variations in nutrient concentrations in Sanriku coastal waters, Japan: Effects on *Undaria pinnatifida* (Laminariales; Phaeophyta) seaweed farms. Reg Stud Mar Sci 54:102484
Kakehi S, Naiki K, Kodama T, Wagawa T, Kuroda H, Ito SI (2018) Projections of nutrient supply to a wakame (*Undaria pinnatifida*) seaweed farm on the Sanriku Coast of Japan. Fish Oceanogr 27:323–335
Kaneda A, Takeoka H, Nagaura E, Koizumi Y (2002) Periodic intrusion of cold water from the Pacific Ocean into the bottom layer of the Bungo Channel in Japan. J Oceanogr 58:547–556
Kato T, Nakahisa Y (1962) A comparative study on two local forms of *Undaria pinnatifida* Sur., a brown alga grown in a culture ground. Bull Jpn Soc Sci Fish 28:998–1004 (in Japanese with English abstract)
Kato S, Dan A (2010) Growth and morphological variations of *Undaria pinnatifida* cultivated in Naruto Strait using seedlings derived from eight areas in Japan. Algal Resources 3:19–26 (in Japanese with English abstract)
Kitadai Y, Kadowaki S (2004) The growth process and N, P uptake rates of *Undaria pinnatifida* cultured in coastal fish farms. Aquacult Sci 52:365–374 (in Japanese with English abstract)
Kobayashi S, Fujiwara T (2009) Modeling the long-term variability of shelf water intrusion into the Seto Inland Sea, Japan. J Mar Syst 77:341–349
Leng Q, Guo X, Zhu J, Morimoto A (2023) Contribution of open ocean to the nutrient and phytoplankton inventory in a semi-enclosed coastal sea. Biogeosciences 20:4323–4338
Makino K, Sumitomo T, Nakanishi T, Kato S, Hirano T, Ueta Y (2015) Mechanism and countermeasures against discoloration of cultured wakame *Undaria pinnatifida*. Aquabiology 37:254–255 (in Japanese with English abstract)
Morita T, Kurashima A, Maegawa M (2003) Temperature requirements for the growth of young sporophytes of *Undaria pinnatifida* and *Undaria undarioides* (Laminariales, Phaeophyceae). Phycol Res 51:266–270
Murase N, Tanada N, Tada A, Shimabukuro H, Yoshida G, Abe M, Noda M (2021) The growth characteristic under high water temperature of young sporophyte of intraspecific crossbreeding of *Undaria pinnatifida* (Laminariales, Phaeophyta) between Naruto cultivar and Tsubaki natural strain, Tokushima Prefecture, Japan. J Nat Fish Univ 69:81–88 (in Japanese with English abstract)
Nagai T, Hibiya T (2012) Numerical simulation of tidally induced eddies in the Bungo Channel: A possible role for sporadic Kuroshio-water intrusion (*kyucho*). J Oceanogr 68:797–806
Nanba N, Fujiwara T, Kuwano K, Ishikawa Y, Ogawa H, Kado R (2011) Effect of water flow velocity on growth and morphology of cultured *Undaria pinnatifida* sporophytes (Laminariales, Phaeophyceae) in Okirai Bay on the Sanriku coast, Northeast Japan. J Appl Phycol 23:1023–1030
Nishijima W (2018) Management of nutrients concentrations in the Seto Inland Sea. Bull Coast Oceanogr 56:13–19 (in Japanese with English abstract)
Nishikawa H (1967) Studies on the "Wakame", *Undaria pinnatifida*, culture in the Ariake Sea-V Estimation of growth and bleaching tips. Aquacult Sci 14:197–203 (in Japanese)
Nishikawa T, Hori Y, Nagai S, Miyahara K, Nakamura Y, Harada K, Tanda M, Manabe T, Tada K (2010) Nutrient and phytoplankton dynamics in Harima-Nada, eastern Seto Inland Sea, Japan during a 35-year period from 1973 to 2007. Estuar Coast 33:417–427
Niwa K (2016) Seedling production of *Undaria pinnatifida* using free-living gametophytes in a large indoor tank. Aquacul Sci 64:173–182 (in Japanese with English abstract)
Niwa K, Kobiyama A (2019) Development of a new cultivar with high yield and high-temperature tolerance by crossbreeding of *Undaria pinnatifida* (Laminariales, Phaeophyta). Aquaculture 506:30–34
Noda M, Murase N (2021) Characteristics of bite scars observed in the cultured wakame *Undaria pinnatifida* by the Japanese black seabream *Acanthopagrus schlegelii* and feeding behavior. J Nat Fish Univ 69:93–101 (in Japanese with English abstract)
Noda M, Murase N (2022) Characteristics of bite scars observed in the cultured wakame *Undaria pinnatifida* by the black scraper *Thamnaconus modestus* and feeding behavior. J Nat Fish Univ 70:115–123 (in Japanese with English abstract)
R Core Team (2021) R: A language and environment for statistical computing. R Foundation for Statistical Computing, Vienna URL http://www.R-project.org/. Accessed 15 Feb 2021

Ross FW, Boyd PW, Filbee-Dexter K, Watanabe K, Ortega A, Krause-Jensen D, Lovelock C, Sondak CFA, Bach LY, Duarte CM, Serrano O, Beardall J, Tarbuck P, Macreadie PI (2023) Potential role of seaweeds in climate change mitigation. Sci Total Environ 885:163699

Sasaki H, Kurihara K, Takayabu I, Uchiyama T (2008) Preliminary experiments of reproducing the present climate using the non-hydrostatic regional climate model. SOLA 4:25–28

Sato Y, Hirano T, Niwa K, Suzuki T, Fukunishi N, Abe T, Kawano S (2016) Phenotypic differentiation in the morphology and nutrient uptake kinetics among *Undaria pinnatifida* cultivated at six sites in Japan. J Appl Phycol 28:3447–3458

Sato Y, Fujiwara T, Endo H (2023) Density regulation of aquaculture production and its effects on commercial profit and quality as food in the cosmopolitan edible seaweed *Undaria pinnatifida*. Front Mar Sci 10:1085054

Spillias S, Valin H, Batka M, Sperling F, Havlík P, Leclère D, Cottrell RS, O'Brien KR, McDonald-Madden E (2023) Reducing global land-use pressures with seaweed farming. Nat Sustain 6:380–390

Stuart MD (1997) Seasonal ecophysiology of *Undaria pinnatifida*. p 193 PhD thesis, University of Otago, Dunedin

Sultana F, Wahab MA, Nahiduzzaman M, Mohiuddin M, Iqbal MZ, Shakil A, Muman AA, Khan MSR, Wong L, Asaduzzaman M (2023) Seaweed farming for food and nutritional security, climate change mitigation and adaptation, and women empowerment: A review. Aquac Fish 8:463–480

Suzuki A, Endo H, Inomata E, Agatsuma Y, Aoki M (2019) Possible use of blue light in *Undaria pinnatifida* aquaculture. J Integr Field Sci 16:12

Takenaka S, Kohno Y, Tamura T, Sakaguchi H, Takechi A, Shimabukuro H, Yoshida G (2021) Growth of *Sargassum fusiforme*, *Undaria pinnatifida* and *Meristotheca papulosa* when cultivated in different water temperature conditions from the Seto Inland Sea to Bungo Channel. Nippon Suisan Gakk 87:375–385 (in Japanese with English abstract)

Takeoka H (2002) Progress in Seto Inland Sea research. J Oceanogr 58:93–107

Tanada N (2016) Development of a practical method for mass seedling production using free-living gametophytes and a new cultivar tolerant to warm waters for early harvesting of *Undaria pinnatifida* (Harvey) Suringar. Aquabiology 225:464–471 (in Japanese with English abstract)

Tanada N, Dan A, Kusaka K, Oka N, Hamano T (2015) A new practical method for mass seedling production of *Undaria pinnatifida* (Harvey) Suringar using free-living gametophytes that originated from single zoospores and its application for commercial cultivation. Algal Resources 8:23–36 (in Japanese with English abstract)

Tanada N, Tada A, Tezuka N, Kiyomoto S (2019) First successful shooting of fish feeding on seedlings of *Undaria pinnatifida* in an aquaculture farm. Tokushima Suikendayori 109:5–7 (in Japanese)

Torres AI, Gil MN, Esteves JL (2004) Nutrient uptake rates by the alien alga *Undaria pinnatifida* (Phaeophyta) (Nuevo Gulf, Patagonia, Argentina) when exposed to diluted sewage effluent. Hydrobiologia 520:1–6

Troell M, Henriksson PJ, Buschmann AH, Chopin T, Quahe S (2023) Farming the ocean –Seaweeds as a quick fix for the climate? Rev Fish Sci Aquac 31:285–295

Usui N, Wakamatsu T, Tanaka Y, Hirose N, Toyoda T, Nishikawa S, Fuji Y, Takatsuki Y, Igarashi H, Nishikawa H, Ishikawa Y, Kuragano T, Kamachi M (2017) Four-dimensional variational ocean reanalysis: a 30-year high-resolution dataset in the western North Pacific (FORA-WNP30). J Oceanogr 73:205–233

Wang L, Park YJ, Jeon YJ, Ryu B (2018) Bioactivities of the edible brown seaweed, *Undaria pinnatifida*: A review. Aquaculture 495:873–880

Watanabe M, Suzuki T, O'ishi R, Komuro Y, Watanabe S, Emori S, Takemura T, Chikira M, Ogura T, Sekiguchi M, Takata K, Yamazaki D, Yokohata T, Nozawa T, Hasumi H, Tatebe H, Kimoto M (2010) Improved climate simulation by MIROC5: mean states, variability, and climate sensitivity. J Clim 23:6312–6335

Yamaguchi A (2010) Biological aspects of herbivorous fishes in the coastal areas of western Japan. Bull Fish Res Agen 32:89–94

Yamamoto T (2003) The Seto Inland Sea-eutrophic or oligotrophic? Mar Pollut Bull 47:37–42

Yamanaka R, Akiyama K (1993) Cultivation and utilization of *Undaria pinnatifida* (wakame) as food. J Appl Phycol 5:249–253

Yanagi T (2015) Oligotrophication in the Seto Inland Sea. In: Yanagi T (ed) Eutrophication and oligotrophication in Japanese estuaries: The present status and future tasks. Springer, Dordrecht, pp 39–67

Yanagi T, Ishii D (2004) Open ocean originated phosphorus and nitrogen in the Seto Inland Sea, Japan. J Oceanogr 60:1001–1005

Yoshida G, Niimura Y, Tarutani K, Hamaguchi M (2011) Research review on the relationship between macroalgal-production and nutrients, and relative assessment of the nutrient conditions on macroalgae in the Seto Inland Sea. Bull Fish Res Agen 34:1–31 (in Japanese with English abstract)

Yoshida G, Shimabukuro H, Kiyomoto S, Kadota T, Yoshimura T, Murase N, Noda M, Takenaka S, Kono Y, Tamura T, Tanada N, Yu X, Yoshie N, Guo X (2019) Assessment and future prediction of climate change impacts on the macroalgal bed ecosystem and cultivation in the Seto Inland Sea. Bull Jap Fish Res Edu Agen 49:27–34

Yoshikawa T, Takeuchi I, Furuya K (2001) Active erosion of *Undaria pinnatifida* Suringar (Laminariales, Phaeophyceae) mass-cultured in Otsuchi Bay in northeastern Japan. J Exp Mar Biol Ecol 266:51–65

Zhang J, Wu W, Ren JS, Lin F (2016) A model for the growth of mariculture kelp *Saccharina japonica* in Sanggou Bay, China. Aquacult Environ Interact 8:273–283